Journal of New Technology and Materials (JNTM)
J. New Technol. Mater.
Vol. 10, N°02 (2020)47-54

OEB Univ. Publish. Co.

Spatial distribution of natural radioactivity and statistical analyses of radioactive variables in Algerian ceramic products

Esma Saadi[a], Ahmed Azbouche[b] and Fatima Benrachi[a]

[a]*Mathematical and Subatomic Physics Laboratory, Frères Mentouri Constantine 1 University, Algeria*

[b]*Nuclear Research Center of Algiers, 02 Bd Frantz Fanon, BP 399, Algiers-Algeria*

*Corresponding author, email: asmasaadi.25@outlook.fr

Received date: Feb. 17, 2020 ; revised date: Oct. 20, 2020; accepted date: Oct. 25, 2020

Abstract

Algerian dwellings are known for their use of ceramics as decorative materials. The latter are mainly composed of clay that contains naturally occurring radionuclides, mainly Uranium and Thorium families and the radioactive isotope of Potassium. Therefore ceramics are classified as a source of hazardous contamination and broad investigations of natural radioactivity levels must be established with the aim of estimating the harmful effects of ionizing radiations emitted by these materials. In this study, thirteen samples collected from ceramic dealers and construction sites were analyzed using a high-resolution HPGe semiconductor detector. Activity concentrations of ^{226}Ra, ^{232}Th and ^{40}K were found with mean specific activities of 22.28±0.61, 29.39±1.34 and 558.31±11.58 Bq.kg^{-1}, respectively. The obtained data were below the recommended values for ^{226}Ra and ^{232}Th. However, they were above them for ^{40}K. Radiological hazards parameters such as radium equivalent, activity concentration index and activity utilization index were calculated and compared to the worldwide average values. Further, statistical analyses were performed and discussed for the resulted data.

Keywords: ceramics; radioactive isotope; specific activities; radium equivalent; statistical analyses.

1. Introduction

Human population has been always exposed to ionizing radiations coming from different sources. The largest contribution to the received collective effective dose is the natural sources [1] that can be originated from cosmic rays and primordial radionuclides. Terrestrial radionuclides such us Potassium, Uranium and Thorium form a large cations which require minerals with large crystal structure openings to fit into. Such minerals are most common in certain types of rocks evolved through different processes in the earth crust [2]. Clay is classified as one of the highest radioactive elements content rocks [3] since it contains mainly silica and alumina besides impurities such as iron, magnesia salts, alkalis (sodium hydroxide Na_2O and potash K_2O), titanium TiO_2, organic materials...etc. [4].

Some construction materials often referred to as naturally occurring radioactive materials (NORM) are mainly constructed using clay such as tiles and bricks. Therefore, they contain primordial radionuclides, like uranium (^{238}U), thorium (^{232}Th) and actinium (^{235}U) series besides potassium (^{40}K). The segment of uranium decay chain starting from radium is the most important from the radiological point of view. Hence, radium is often made as a reference instead of uranium [5]. These terrestrial radionuclides contribute to the major part of the natural radioactivity dose rate as most of the people spend approximately 80-90% of their time indoors [6], they pose external exposure risks caused by their gamma-ray emissions and internal ones due to the inhalation of the radioactive inert gas radon (^{222}Rn) and its short-lived decay products [7].

The main objective of this research work is to examine the activity concentrations of terrestrial radionuclides ^{226}Ra, ^{232}Th and ^{40}K in thirteen Algerian ceramic samples that are commonly used in dwellings, by means of a high-resolution coaxial hyper-pure germanium detector. In the aim to assess, the potential radiological risks related to the use of such materials on inhabitant health, some radiological hazard indices were calculated based on the specific activities of the terrestrial radionuclides ^{226}Ra, ^{232}Th and ^{40}K. Such as radium equivalent activity (Ra_{eq}), activity concentration index (I) and activity utilization index (AUI). Descriptive statistics were also determined to illustrate the distribution of the natural isotopes in the studied samples.

2. Materials and methods

2.1. Sample collection and preparation

Thirteen samples of the current study were collected from ceramic dealers and construction sites: CA1 and CA2 from Algiers, CA3 from Annaba, CB1 and CB2 from Batna, CB3 from Béjaïa, CB4 and CB5 from Bordj Bou Arreridj, CB6 from Biskra, CC1 from Constantine, CC2 from Chelghoum El Laïd, CM1 from Mascara and CT1 from Tipaza (Figure 1). The samples were crushed and milled into a fine powder, and then they were dried in an oven under a temperature of 110 °C for at least 24

hours in a way to remove the moisturizing content and obtain a constant weight. The samples were conditioned in thin Plexiglas boxes to avoid the self-absorption of low energy gamma. These boxes were carefully sealed for a period of four weeks (~ 7 half-lives) to ensure secular equilibrium between radon emitted by the samples and the one originated from environment during the samples preparation, in other words, in the period of four weeks all radon contamination will be eliminated.

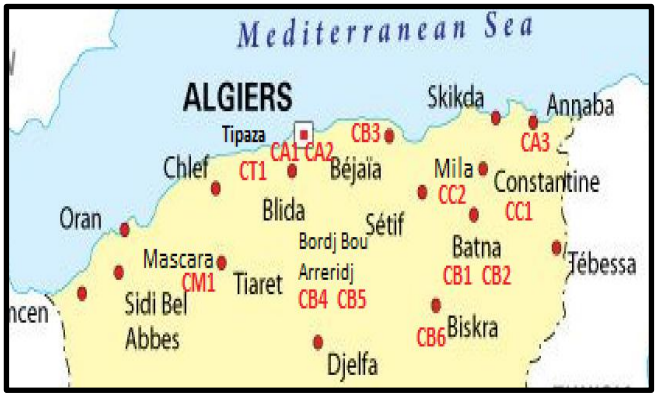

Figure 1. Map of the samples.

2.2. Experimental method for gamma spectroscopy

The measurements were carried out by means of a P-type coaxial Canberra, with 40% relative efficiency, to determine the activities of different radioactive isotopes present in the samples. It is expected to measure the natural radionuclides such as ^{238}U and ^{232}Th decay chains, ^{40}K and possibly ^{137}Cs radioisotope of human origin. The detector is surrounded by 11.4-cm-thick graded lead shield (Canberra 7477 Series Lead Shield) with liners of 1.5 mm of copper and 3mm of tin to reduce X-ray fluorescence from lead shield. The gamma-energy photo-peak resolution of the gamma spectrometry system is 0.86 keV at 122 keV for ^{57}Co and 1.85 keV at 1332.5 keV for ^{60}Co. The detector efficiency calibration was performed using a liquid source of ^{152}Eu mixed with water matrix. The detector efficiency values were calculated by Monte Carlo simulation using MCNP5 code [8, 9] taking into account the coincidence summing effects on efficiency calibration. Figure 2 shows the fitted efficiency curve of the detector as a function of gamma rays energy. The Genie 2000 software packages were used for the acquisition and treatment of the collected data. Each sample was measured for at least 24 hours to obtain the γ-spectrum with good statistics. The ^{234}Th (63 keV) gamma-ray transition was used to determine the concentration of ^{238}U, the gamma-ray transitions of energies ^{214}Pb (352 keV) keV and ^{214}Bi (609 keV) were used to determine the activity concentration of ^{226}Ra. The gamma-ray transitions of energies ^{228}Ac (911 keV), ^{208}Tl (583 keV), ^{212}Pb (239 keV) and ^{212}Bi (727 keV) were used to determine the activity concentration of ^{232}Th and the ^{40}K (1461 keV) gamma-ray transition was used to determine the concentration of ^{40}K in different samples. Specific Activity of each individual radionuclide in ceramic samples was determined using the relation 1, taking into account the net peak area N_{Ej} of a photopeak at energy E_j, the absolute full energy peak detection efficiency ε_{Ej}, the gamma-ray emission probability P_{Ej}, the counting time t_c and the mass of the measured sample m.

$$A_{Ej}(Bq/kg) = N \frac{N_{Ej}}{\varepsilon_{Ej} \times P_{Ej} \times t_c \times m} \quad (1)$$

The activity concentration of ^{40}K was calculated directly using relation 1. While, the ^{226}Ra and ^{232}Th ones were obtained from calculated specific activities of their radioactive descendants A_{Ej} within the assumption of equilibrium at a photopeak at energy E_j by the following equation.

$$A_i(Bq/kg) = \frac{1}{n}\sum_j^n A_{Ej} \quad (2)$$

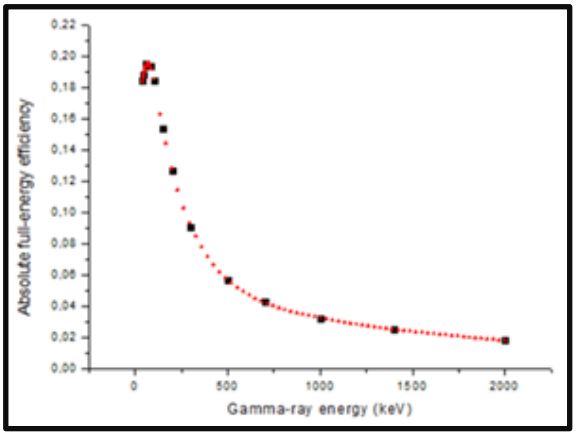

Figure 2. Efficiency curve as a function of energies.

3. Results and discussion

3. 1. Levels of activity concentrations

The activity concentrations of the different ceramic samples are reported in Table 1. They range from 15.19±0.60 to 29.04±0.69 Bq.kg^{-1}, from 20.36±1.11 to 40.22±1.65 Bq.kg^{-1} and from 311.32±8.88 to 790.78±13.32 Bq.kg^{-1} with mean specific activities 22.28±0.61, 29.39±1.34 and 558.31±11.58 Bq.kg^{-1} for ^{226}Ra, ^{232}Th and ^{40}K, respectively. According to the European recommendations and based on a literature study [10, 11], the worldwide average values for ^{226}Ra, ^{232}Th and ^{40}K are 40, 40 and 400 Bq.kg^{-1}, respectively. The results of this study are below the recommended values for ^{226}Ra and ^{40}K in all samples. In the case of ^{40}K, they are higher than the global average in all samples except CB2, CB6 and CC2. It is obvious from the results displayed in figure 3 that sample CA2 contains the highest activity concentrations ^{40}K and sample CB1 has the highest specific activities of ^{226}Ra and ^{232}Th. However, sample CA3 has the lowest activity concentration of ^{226}Ra, sample CM1 has the lowest specific activity of ^{232}Th and sample CB2 contains the lowest activity concentration of ^{40}K. These differences in the activity

concentrations of primordial radionuclides among ceramic samples can be attributed to the dissimilarities in the clay's mineral composition of each sample which differ from one region to another depending on the geological nature. Moreover, it is noticed that there is an absence of artificial radionuclides in the studied samples, which means that the sampling sites do not present any anthropogenic contamination.

Table 1: Mean activity concentrations for different samples.

Samples		^{226}Ra (Bq.kg^{-1})	^{232}Th (Bq.kg^{-1})	^{40}K (Bq.kg^{-1})
Origin	Code			
Algiers	CA1	22.45±0.61	30.23±1.61	643.18±12.43
Algiers	CA2	28.50±0.68	39.04±1.31	790.78±13.32
Annaba	CA3	15.19±0.60	26.73±1.39	583.81±12.30
Batna	CB1	29.04±0.69	40.22±1.65	773.34±13.05
Batna	CB2	18.90±0.56	23.94±1.07	311.32±8.88
Béjaïa	CB3	21.64±0.65	33.27±1.40	654.7±12.78
Bordj Bou Arreridj	CB4	25.60±0.68	39.23±1.54	724.29±13.47
Bordj Bou Arreridj	CB5	16.99±0.56	31.87±1.39	561.05±11.90
Biskra	CB6	15.67±0.49	20.63±1.12	358.75±9.74
Constantine	CC1	23.81±0.65	27.79±1.36	418.86±10.54
Chelghoum El Laïd	CC2	24.05±0.57	23.42±1.12	382.96±9.47
Mascara	CM1	23.83±0.62	20.36±1.11	501.88±10.80
Tipaza	CT1	23.97±0.64	25.34±1.33	553.06±11.88
Average		22.28±0.61	29.39±1.34	558.31±11.58
Worldwide		40	40	400

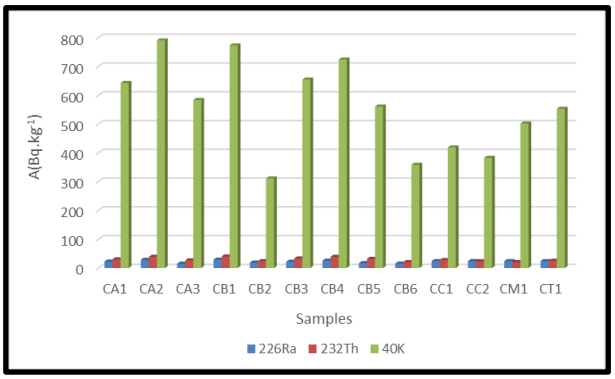

Figure 3. Activity concentrations of ^{226}Ra, ^{232}Th and ^{40}K in the studied samples.

3. 2. Correlation studies and activity ratios

In order to find extent of ^{226}Ra, ^{232}Th and ^{40}K together at a particular place, correlation studies were made between them as it is shown in Figure 4. It can be clearly noticed that there is a low correlation between (^{226}Ra, ^{232}Th) and (^{226}Ra, ^{40}K) pairs in ceramic samples, where the correlations coefficients are R^2= 0.3229 and R^2=0.3218, respectively. Nevertheless, there is a high correlation between (^{232}Th, ^{40}K) pair with a correlation coefficient R^2=0.7616. This strong correlation indicates that the individual result is a good predictor for the concentration of the other component of the pair [12, 13]. Table 2 shows activity concentrations ratios of ^{226}Ra, ^{232}Th and ^{40}K for the measured samples. The results show that all the ^{232}Th/^{40}K and ^{226}Ra/^{40}K ratios are below unity, which means that the ^{40}K activity concentrations are higher than those of ^{226}Ra and ^{232}Th in these samples. Moreover, all the samples have ^{232}Th/^{226}Ra ratios above unity except samples CB6 and CM1, which indicate that the ceramic products are enriched in ^{232}Th more than ^{226}Ra.

3. 3. Radium equivalent (Raeq)

The distributions of ^{226}Ra, ^{232}Th and ^{40}K are not uniform in the samples. Hence, Radium equivalent (Ra_{eq}) has been introduced to estimate the actual activity level of these radionuclides and to assess the radiation hazards associated with their presence in building materials [14]. It is defined by equation 3 [15, 5].

$$Ra_{eq} = A_{Ra} + +1.43A_{Th} + 0.077A_K \quad (3)$$

Where A_{Ra}, A_{Th}, and A_K, are specific activities of ^{226}Ra, ^{232}Th, and ^{40}K, respectively in Bq.kg^{-1}. The base estimation of this formula is that 1 Bq.kg^{-1}of ^{226}Ra, 0.7 Bq.kg^{-1}of ^{232}Th and 13 Bq.kg^{-1}of ^{40}K produce the same γ-ray dose rate [16, 17].

The Ra_{eq} calculated values are reported in table 4 and presented in Figure 5; they lie from 72.79±1.84 Bq.kg^{-1} to 146.1±2.66 Bq.kg^{-1}, with an average value of 107.30±2.20 Bq.kg^{-1} in ceramic samples. The latter are within the permissible limit of 370 Bq.kg^{-1} [5].

3. 4. Activity concentration index (I)

According to the European commission [10], if the excess gamma radiation originating from construction materials increases the annual effective dose of a member of the public by 0.3 mSv at the most, they should be exempted from all restrictions concerning their radioactivity. On the other hand, doses exceeding the dose criterion of 1 mSv should be accepted only in few cases where materials are used locally [18]. Hence, it is

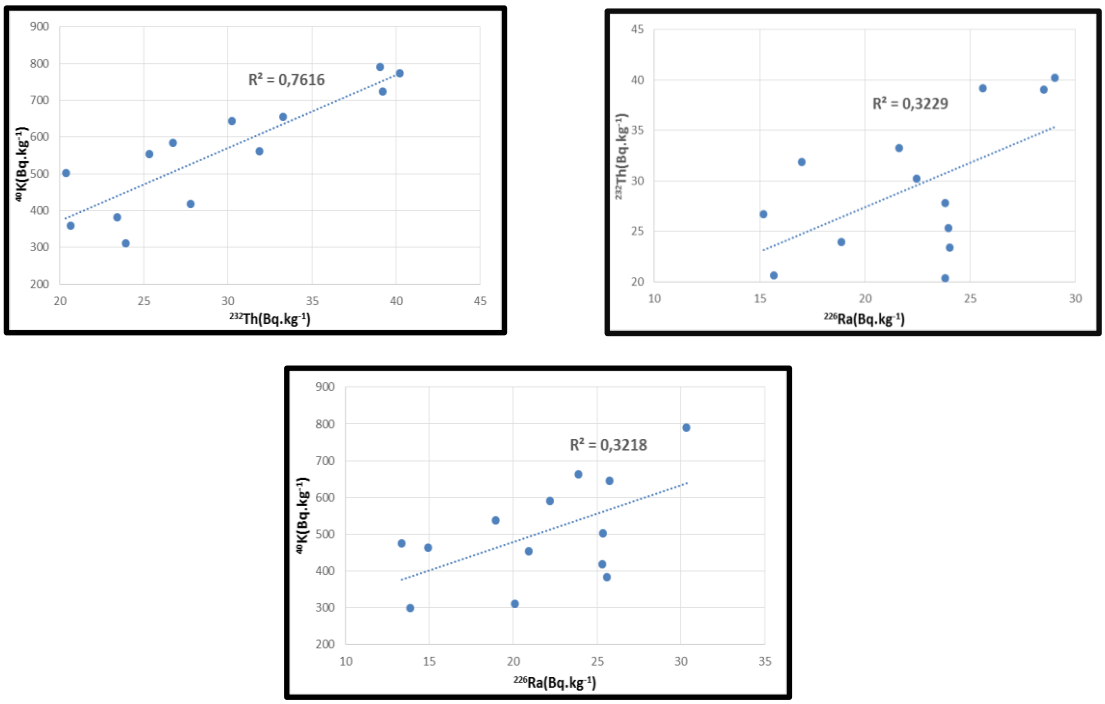

Figure 4. Correlation between activity concentrations of natural radionuclides in the investigated samples.

Table 2: Activity ratios of ^{226}Ra, ^{232}Th and ^{40}K.

Samples		Activity ratios		
Origin	Code	^{232}Th/^{226}Ra	^{232}Th/^{40}K	^{226}Ra/^{40}K
Algiers	CA1	1,35	0.05	0.03
Algiers	CA2	1.37	0.05	0.04
Annaba	CA3	1.76	0.05	0.03
Batna	CB1	1.38	0.05	0.04
Batna	CB2	1.27	0.08	0.06
Béjaïa	CB3	1.54	0.05	0.03
Bordj Bou Arreridj	CB4	1.53	0.05	0.04
Bordj Bou Arreridj	CB5	1.88	0.06	0.03
Biskra	CB6	1.32	0.06	0.04
Constantine	CC1	1.17	0.07	0.06
Chelghoum El Laïd	CC2	0.97	0.06	0.06
Mascara	CM1	0.85	0.04	0.05
Tipaza	CT1	1.06	0.05	0.04
Mean		1.34	0.05	0.04

recommended that controls should be based on a dose range 0.3-1 mSv.y^{-1}, which is the excess gamma dose contribution to the dose received outdoors [19]. The activity concentration index can be calculated using formula 4 [10].

$$I = \frac{A_{Ra}}{300\ Bq/kg} + + \frac{A_{Th}}{200\ Bq/kg} + \frac{A_K}{3000\ Bq/kg} \quad (4)$$

Where A_{Ra}, A_{Th} and A_K are specific activities of ^{226}Ra, ^{232}Th and ^{40}K, respectively. The activity concentration index shall not exceed the values shown in table 3.

Activity concentration index values of the ceramic samples were calculated. The results are shown in Table 4 and displayed in Figure 6. They range from 0.27 to 0.56 with a mean value of 0.41 which is under both of the recommended lower limit of I ≤ 0.5 for materials used in bulk amounts and I ≤ 2 for superficial and other materials with restricted use (Table 3). As a result, the annual effective dose delivered by the studied ceramic samples is smaller than the annual effective dose limit of 0.3 mSv.

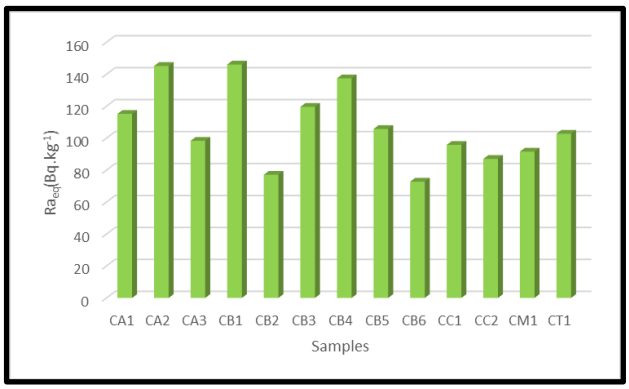

Figure 5. Radium equivalent (Ra_{eq}) for ceramic samples.

Table 3: Maximum recommended values of activity concentration index depending on the dose criterion, and the way and the amount the material is used in a building.

Dose criterion	0.3 mSv.y^{-1}	1 mSv.y^{-1}
Materials used in bulk amounts, e.g. concrete	I	I ≤ 1
Superficial and other materials with restricted use: tiles, boards, etc.	I	I ≤ 6

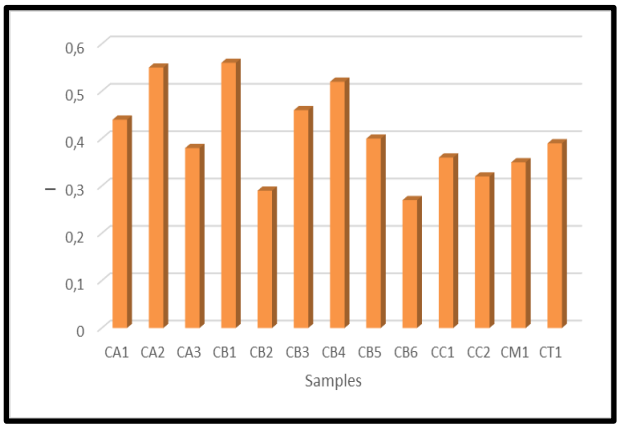

Figure 6. Activity concentration index (I) for samples under investigation.

Activity utilization index (AUI) can be determined by applying the suitable conversion factors with dose rates in air from different combinations of ^{226}Ra, ^{232}Th and ^{40}K in the studied samples. It can be calculated using equation 5 [20].

$$AUI = \frac{A_{Ra}}{50Bq/kg} f_{Ra} + \frac{A_{Th}}{50Bq/kg} f_{Th} + \frac{A_K}{500Bq/kg} f_K \qquad (5)$$

Where C_{Ra}, C_{Th} and C_K are the specific activities of ^{226}Ra, ^{232}Th and ^{40}K in Bq.kg^{-1}, respectively. f_{Ra} (0.462), f_{Th} (0.604) and f_K (0.042) are the respective fractional contributions from the actual activities of ^{226}Ra, ^{232}Th, and ^{40}K to the total dose rate in air [21]. As can be seen in Table 4 and perceived from Figure 7, the calculated values of AUI vary from 0.42 to 0.82 with a medium value of 0.61. The resulted data in this study are less than the recommended value of 2 which corresponds to an annual effective dose <0.3 mSv.y^{-1} [19].

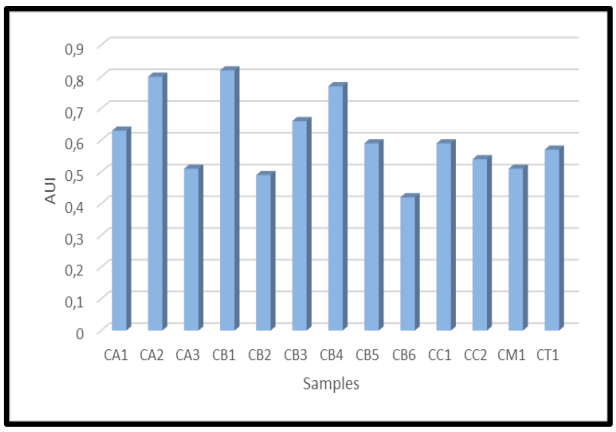

Figure 7. Activity utilization index (AUI) for the studied samples.

3. 5. Activity utilization index (AUI)

TABLE 4. Calculated radiological risk indices.

Samples	Ra_{eq}(Bq.kg^{-1})	I	AUI
CA1	115.22±2.57	0.44±0.27	0.63±0.02
CA2	145.21±2.24	0.55±0.34	0.80±0.02
CA3	98.37±2.16	0.38±0.24	0.51±0.02
CB1	146.10±2.66	0.56±0.34	0.82±0.02
CB2	77.11±1.77	0.29±0.17	0.49±0.01
CB3	119.63±2.33	0.46±0.28	0.66±0.02
CB4	137.47±2.52	0.52±0.32	0.77±0.02
CB5	105.77±2.26	0.40±0.25	0.59±0.02
CB6	72.79±1.84	0.27±0.17	0.42±0.01
CC1	95.80±2.20	0.36±0.21	0.59±0.02
CC2	87.03±1.85	0.32±0.19	0.54±0.01
CM1	91.58±1.90	0.35±0.21	0.51±0.01
CT1	102.79±2.20	0.39±0.24	0.57±0.02
Average	107.30±2.20	0.41±0.25	0.61±0.02
Worldwide	370	1	2

3.6. Statistical analyses of the data

In statistics, histogram is a graphical representation of the distribution of data. The frequency distribution of ^{226}Ra, ^{232}Th and ^{40}K activity concentrations in ceramic samples were analyzed, where the histograms are given in Figure 8. The graphs show that all radioactive variables exhibited some degree of multi-modality, which demonstrate that ceramic composition vary from one region to another.

Table 5 displays the values of different descriptive statistics such as mean, standard deviation (σ), variance, kurtosis, skewness, range, minimum and maximum. Which were calculated for the concentrations of natural radioisotopes ^{226}Ra, ^{232}Th and ^{40}K for the investigated samples. It can be clearly noticed that the values of the standard deviation are lower than the mean values of primordial radionuclides, which indicates the high degree of consistency of their distribution in ceramic samples. It is also observed that the radioactive variables show a lower order of variance for ^{226}Ra and ^{232}Th which implies a higher degree of homogeneity and a lower degree of mobility, hence. They show a higher order of variance for ^{40}K indicating a lower degree of homogeneity and a higher degree of mobility [22]. Kurtosis is a characterization of the relative flatness of a distribution; the results of ^{226}Ra, ^{232}Th and ^{40}K show a negative kurtosis indicating a relatively flat distribution [22]. The degree of asymmetry of real valued haphazard variable distribution can be characterized by means of skewness [22, 23]. The results of this study show positive skewness value for ^{232}Th, which explain the asymmetric tail extending towards values that are more positive in its distribution, however. The results show a negative skewness values for ^{226}Ra and ^{40}K explaining the asymmetric tail extending towards values that are more negative in the their distributions.

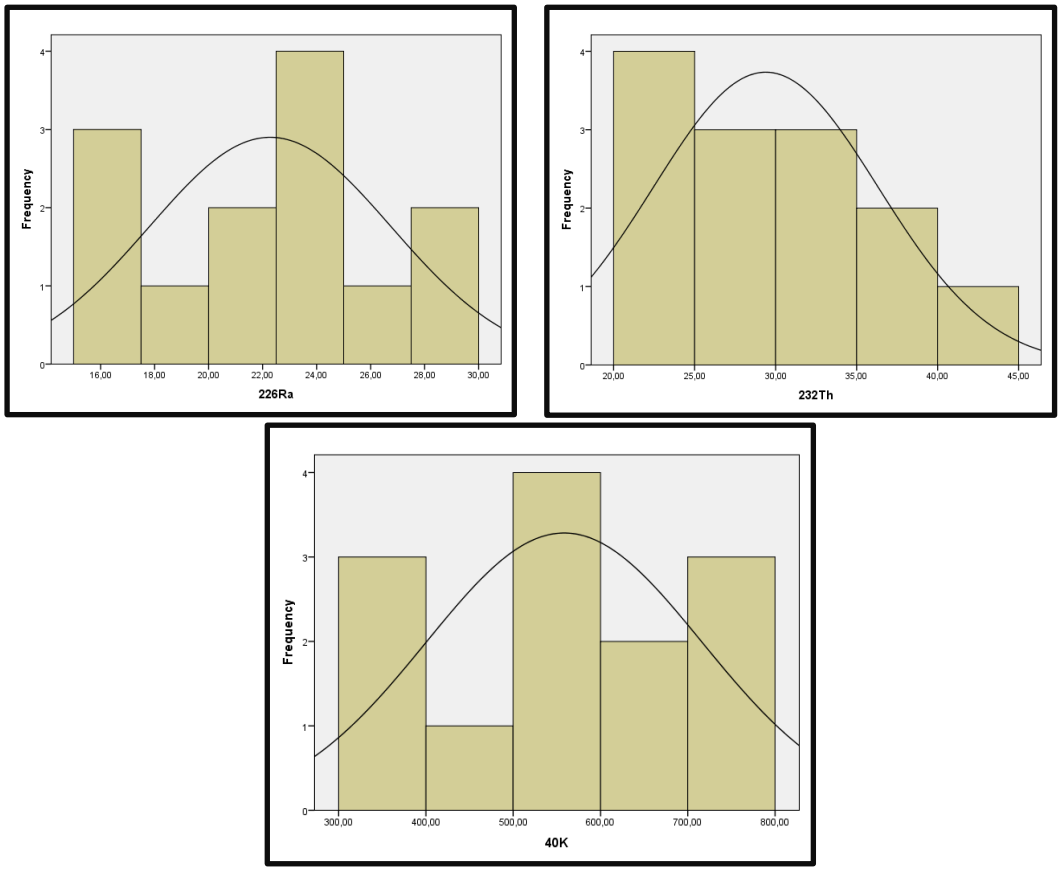

Figure 8. Frequency distributions of ^{226}Ra, ^{232}Th and ^{40}K for the studied samples.

Table 5: Descriptive statistics for concentrations of natural radionuclides ^{226}Ra, ^{232}Th and ^{40}K in ceramic samples

Radionuclides Concentrations (Bq.kg^{-1})	Descriptive statistics			
	Mean	Σ	Variance	Kurtosis
^{226}Ra	22.28	4.47	20	-0.79
^{232}Th	29.39	6.95	48.23	-1.14
^{40}K	558.31	157.91	24934.61	-1.13
	Skewness	Range	Minimum	Maximum
^{226}Ra	-0.25	13.85	15.19	29.04
^{232}Th	0.39	19.86	20.36	40.22
^{40}K	-0.07	479.46	311.32	790.78

4. Conclusion

The activity concentrations of the naturally occurring radionuclides ^{226}Ra, ^{232}Th and ^{40}K have been measured from thirteen ceramic samples used in Algeria, by means of gamma spectrometry analysis with a high-resolution HPGe detector specific for low gamma energies. They have been found with mean specific activities of 22.28±0.61, 29.39±1.34 and 558.31±11.58 Bq.kg^{-1} for ^{226}Ra, ^{232}Th and ^{40}K, respectively. The obtained data were below the recommended values for ^{226}Ra and ^{232}Th. However, they were above them for ^{40}K. The radium equivalent activity (Ra_{eq}) values lie from 72.79±1.84 Bq.kg^{-1} to 146.1±2.66 Bq.kg^{-1}, which are lower than the worldwide average of 370 Bq.Kg^{-1}. The determined activity concentration index (I) range from 0.27 to 0.56, the resulted values of I are less than the standard mean value of 1, the estimated activity utilization index fluctuates between 0.42 and 0.82 falling under the recommended limits of unity.

From our study, we can conclude that the wide usage of ceramic products should be done with caution as they show high activity concentration of ^{40}K. But still no regulations and restrictions against the usage of these building materials, hence, more samples should be analyzed in order to confirm the results obtained in this study.

References

[1] G. Cinelli, T. Tollefsen, P. Bossew, V. Gruber, K. Bogucarskis, L. De Felice, M. De Cort, "Digital version of the European Atlas of natural radiation", *J. Environ. Radioact, 196 (2019) 240-252.* https://doi.org/10.1016/j.jenvrad.2018.02.008.

[2] B. W. Hurley, "Natural Radioactivity in the Geologic Environment", National nuclear security administration, Nevada site office, CEMP, (2009).

[3] R. Six, (2012). https://robertsix.wordpress.com/2016/02/14/la-radioactivite-des-roches 3/

[4] H. Boussak, "Effet de la température sur les performances des céramiques contenant la bentonite de Maghnia", (Thèse de doctorat). M'Hamed Bougara-Boumerdes University, Algeria (2015).

[5] NEA-OECD, "Exposure to radiation from natural Radioactivity in building materials; report by NEA group of experts". OECD, Paris (1979).

[6] L. Xinwei, "Radioactivity level in Chinese building ceramic tile", Rad. Prot. Dos, 112(2), (2004) 323-327. https://doi.org/10.1093/rpd/nch396.

[7] S. Solak, Ş. Turhan, F A. Ugŭr E. Gören, F. Gezer, Z. Yeğingil and I. Yeğingil, "Evaluation of Potential Exposure Risks of Natural Radioactivity Levels Emitted from Building Materials used in Adana, Turkey", Indoor Built Environ, 000 (2012) 1–9. https://doi.org/10.1177/1420326x12448075

[8] A. Azbouche, M. Belgaid, H. Mazrou, "Monte Carlo calculations of the HPGe detector efficiency for radioactivity measurement of large volume environmental samples", J. Environ. Radioact, 146 (2015) 119–124. https://doi.org/10.1016/j.jenvrad.2015.04.015

[9] A. Azbouche, M. Belamri, T. Tchakoua, "Study of the germanium dead layer influence on HP(Ge) detector efficiency by Monte Carlo simulation", Radiation Detection Technology and Methods, 2 (2018) 45. https://doi.org/10.1007/s41605-018-0074-y

[10] European Commission (EC), "Radiological protection principles concerning the natural radioactivity of building materials", European Commission. Radiation Protection 112. Directorate General, Environment Nuclear Safety and Civil Protection (1999).

[11] R. Mustonen, M. Pennanen, M. Annanmäki, E. Oksanen, "Enhanced Radioactivity of Building Materials", Final report of the contract No 96-ET-003 for the European Commission. Radiation and Nuclear Safety Authority – STUK, Finland, 1997, Radiation Protection 96, Luxembourg (1999).

[12] G. Bouhila, A. Azbouche, F. Benrachi, M. Belamri, "Natural radioactivity levels and evaluation of radiological hazards from Beni Haroun dam sediment samples", Environ. Earth. Sci, 76 (2017) 710. https://doi.org/10.1007/s12665-017-7061-3

[13] S. M. Darwish, S. M. El-Bahi, A. T. Sroor, N. F. Arhoma, "Natural radioactivity assessment and radiological hazards in soils from Qarun Lake and Wadi El Rayan in Faiyum, Egypt", Open Journal of Soil Science, 3 (2013) 289–296. https://doi.org/10.4236/ojss.2013.37034.

[14] K. Vanasundari, R. Ravisankar, D. Durgadevi, R. Kavita, M. Karthikeyan, K. Thillivelvan, B. Dhinakaran, "Measurement of Natural Radioactivity in Building Material Used in Chengam of Tiruvannamalai District, Tamilnadu by Gamma-Ray Spectrometry", Indian J Adv Chem Sci, 1(2012) 22-27. https://doi.org/10.1016/j.jtusci.2015.08.004.

[15] J. Beretka, and P. J. Mattew, "Natural radioactivity of Australian building materials, Industrial wastes and by products", Health Phys, 48(1985) 87-95. https://doi.org/10.1097/00004032-198501000-00007.

[16] E. M. Krisiuk, S. I. Tarasov, V. P. Shamov, N. I. Shalak, E. P. Lisachenko, L. G. Gomelsky, "A Study on Radioactivity in Building Materials" (Leningrad: Research Institute for Radiation Hygiene), (1971).

[17] E. Stranden, "some aspects on radioactivity of building materials", Phys Norv, 8 (1976)167-173.

[18] S. Righi, R. Guerra, M. Jeyapandian, S. Verità, A. Albertazzi, "Natural radioactivity in Italian

ceramic tiles", Radioprotection, 44 (2009) 413–419. https://doi.org/10.1051/radiopro/20095078.

[19] H. El-Gamal, E. Sidique, M. El-Haddad, M. E. Farid, "Assessment of the natural radioactivity and radiological hazards in granites of Mueilha area (South Eastern Desert, Egypt)", Environ. Earth. Sci, 77(2018) 691. https://doi.org/10.1007/s12665-018-7880-x

[20] R. D. Senthilkumar, R. Narayanaswamy, "Assessment of radiological hazards in the industrial effluent disposed soil with statistical analyses", Journal of Radiation Research and Applied Sciences, 9 (2016) 449-456. https://doi.org/10.1016/j.jrras.2016.07.002.

[21] A. Chandrasekaran, R. Ravisankar, G. Senthilkumar, K. Thillaivelavan, B. Dhinakaran, P. Vijayagopal, S. N. Bramha, B. Venkatraman, "Spatial distribution and lifetime cancer risk due to gamma radioactivity in Yelagiri Hills, Tamilnadu, India", Egyptian Journal of Basic and Applied Sciences, 1(2014) 38-48. https://doi.org/10.1016/j.ejbas.2014.02.001

[22] A. M. A. Adam, M. A. H. Eltayeb, "Multivariate statistical analysis of radioactive variables in two phosphate ores from Sudan", J. Environ. Radioact, 107 (2012) 23-43. https://doi.org/10.1016/j.jenvrad.2011.11.021.

[23] R. A. Groeneveld, G. Meeden, "Measuring Skewness and Kurtosis". the Statistician, 4 (1984) 391-399. https://doi.org/10.2307/2987742.